Desalination and Water Treatment
www.deswater.com

17 (2010) 80–89
May

1944-3994/1944-3986
doi: 10.5004/dwt.2010.1702

Effects of high-pressure carbon dioxide on the demulsification of O/W emulsion

Satoshi Nagao[a], Tomoki Takahashi[b]*, Atsushi Shono[b], Katsuto Otake[b]

[a]*Graduate School of Engineering, Tokyo University of Science, Kagurazaka 1-3, Shinjyuku-ku, Tokyo 162-8601, Japan*
[b]*Faculty of Engineering, Tokyo University of Science, Kagurazaka 1-3, Shinjyuku-ku, Tokyo 162-8601, Japan*
Tel. +81332604272 (ext 4720); Fax +81352614631; email: t.takahashi@ci.kagu.tus.ac.jp

Received 31 July 2009; accepted 23 November 2009

A B S T R A C T

A new process for the demulsification of oil-in-water (O/W) emulsion with high-pressure carbon dioxide (CO_2) was proposed. For the confirmation of the concept, demulsification of O/W emulsion formed with a nonionic surfactant, Tween 20, was conducted. The behavior of O/W emulsion under high-pressure CO_2 was examined with a visual observation and an electrical conductivity measurement of the emulsions. Efficiency of the demulsification was evaluated by the oil content of water-rich phases and the amount of water-rich phases separated from the emulsion by the creaming of the oil phases. Experimental results revealed that the high-pressure CO_2 acts as a swelling reagent that lowers the density of the dispersed oil phase to induce the floatation of the oil droplet that leads to an efficient demulsification.

Keywords: Waste water treatment; High-pressure CO_2; O/W emulsion; Flotation

1. Introduction

An emulsion is a dispersion of one liquid in another where each liquid is immiscible, or poorly miscible in the other [1]. This emulsion is divided into two types, oil-in-water (O/W) and water-in-oil (W/O).

In the industrial mass waste water treatment, O/W emulsion needs to be demulsified. Generally, the demulsification is performed by gravitational sedimentation, pressure floatation and membrane separation. The functional declines of surfactants by the addition of electrolytes (e.g. $CaCl_3$, $AlCl_3$) as well as surfactants that have different HLB are also effective [2–4]. However, processing of a large amount of O/W waste water with high performance is very difficult [5].

For the efficient demulsification, we propose a new process that uses high-pressure Carbon dioxide (CO_2) as a demulsification reagent. Considering the CO_2 as a demulsifying reagent, there are two advantages. One is that the CO_2 has high affinity to nonpolar substances such as alkane oils, and dissolves into the oil phase to swell the oil droplets of O/W emulsion which results in the decrease in density. The difference in density between the oil phase and the aqueous phase enhances the demulsification. The other is that the CO_2 dissolves into the water phase to form carbonic acid that acts as an electrolyte. The carbonic acid breaks electric charge balance of O/W emulsion, and the surfactant layer on the oil–water interface becomes unstable.

In this study, demulsification of O/W emulsion formed with a nonionic surfactant, Tween 20 [6], was conducted to confirm the feasibility of the concept described above.

*Corresponding author

Presented at the Fifth Conference of the Aseanian Membrane Society Aseania 2009 "Recent Progress in Membrane Science and Technology", 12–14 July 2009, Kobe, Japan.

2. Experimental

2.1. Materials

n-Decane, *n*-dodecane and *n*-hexadecane were used for the oil phase of O/W emulsions. They were all special grade, and were purchased from Wako pure chemicals, and used as received. Distilled and deionized water, prepared in our laboratory, was used for the aqueous phase of O/W emulsions. Nonionic surfactant polyoxyethylene sorbitan monolaurate (Tween 20) was also supplied from Wako pure chemicals, and used without further treatment. The CO_2 was supplied from the Tomoe Shokai, and was used as received. The purity was 99.99%.

2.2. Experimental condition

All experiments were mainly conducted at 50°C and pressures up to 10 MPa.

2.3. Preparation of emulsions

O/W emulsions were prepared by stirring the mixture of distilled water, Tween 20, and oil using a high-speed homogenizer (ULTRA-TURRAX T-25 Basic, IKA) at 20,000 rpm for 1 h. The mass ratio of water:surfactant:oil was 85:1:14. Surfactant was added to the water before the emulsification. These emulsions were stable within the experimental time range.

2.4. Visual observation of solutions

The demulsification was performed by treating the O/W emulsions with high-pressure CO_2 in a stainless steel high-pressure autoclave that has an optical window. One milliters of samples was placed in the glass cylinder (2.5 mL in volume) that has a scale to measure the change in volume of the sample. Through the window, the behavior of O/W emulsions under high-pressure CO_2 was observed visually. The swelling behavior of aqueous surfactant solution and pure oils were also examined. The change in volume of solutions, especially for oils, was measured, and the expansion coefficient of the oil phase was calculated.

2.5. Electrical conductivity measurement

Generally, stability of emulsions is evaluated with using dynamic light scattering (DLS), turbidity measurement, dielectric constant measurement, and electric conductivity measurement [7–11]. In particular, the electric conductivity of the emulsion is a good measure of the ion concentration as well as the volume ratio of the dispersion phase that has different conductivity with the continuous phase. Electrical conductivity change of the O/W emulsion during the demulsification was measured by an impedance analyzer (HP 4192A, Hewlett Packard) and a plate capacitor with a high-pressure autoclave that has no window. The plate capacitor was set at the bottom of the O/W emulsion sample placed in a glass cup set in the autoclave. The electrical conductivity of the aqueous Tween 20 solution was also measured for comparison.

2.6. Evaluation of demulsification efficiency

The demulsification of O/W emulsion samples (50 g) was measured with an autoclave that has two windows on both sides. As the demulsification proceeds, phase separation of the O/W emulsion occurs to form an upper oil rich phase (i.e., creaming layer) and a lower water rich phase. After the demulsification, the lower phase was separated from the creaming layer with using the pressure difference between inside and outside of the apparatus.

In this study, demulsification efficiency was evaluated by two means: mass fraction of the lower phase to the total mass of the O/W emulsion (X_{under} [wt%]), and mass fraction of the oil in the lower phase (ϕ_{oil} [wt%]). This oil contents in the lower phase was calculated from the heat of melting of the oil in the sampled lower phase obtained from a differential scanning calorimetry (SSC5200, Seiko Instruments Inc.) thermogram as follows:

$$\phi_{\mathrm{oil}}[\mathrm{wt\%}] = \frac{\Delta H_{\mathrm{oil}}}{H_{\mathrm{oil}}} \times 100, \tag{1}$$

$$X_{\mathrm{under}}[\mathrm{wt\%}] = \frac{\text{Mass of lower phase}}{\text{Total mass of emulsion}} \times 100, \tag{2}$$

where ΔH_{oil} [J] is the heat of melting of the oil per gram of the emulsion, and H_{oil} [J/g] is the heat of melting per gram of the oil. As X_{under} represents the amount of the lower phase recovered from the emulsion to the initial emulsion, its maximum value is 86%. When the ϕ_{oil} is low and the X_{under} is high, the demulsification efficiency is high.

3. Results and discussion

3.1. Visual observation

Fig. 1 shows the O/W emulsions of decane (a), dodecane (b) and hexadecane (c) before and after the high-pressure CO_2 treatment for 2 h.

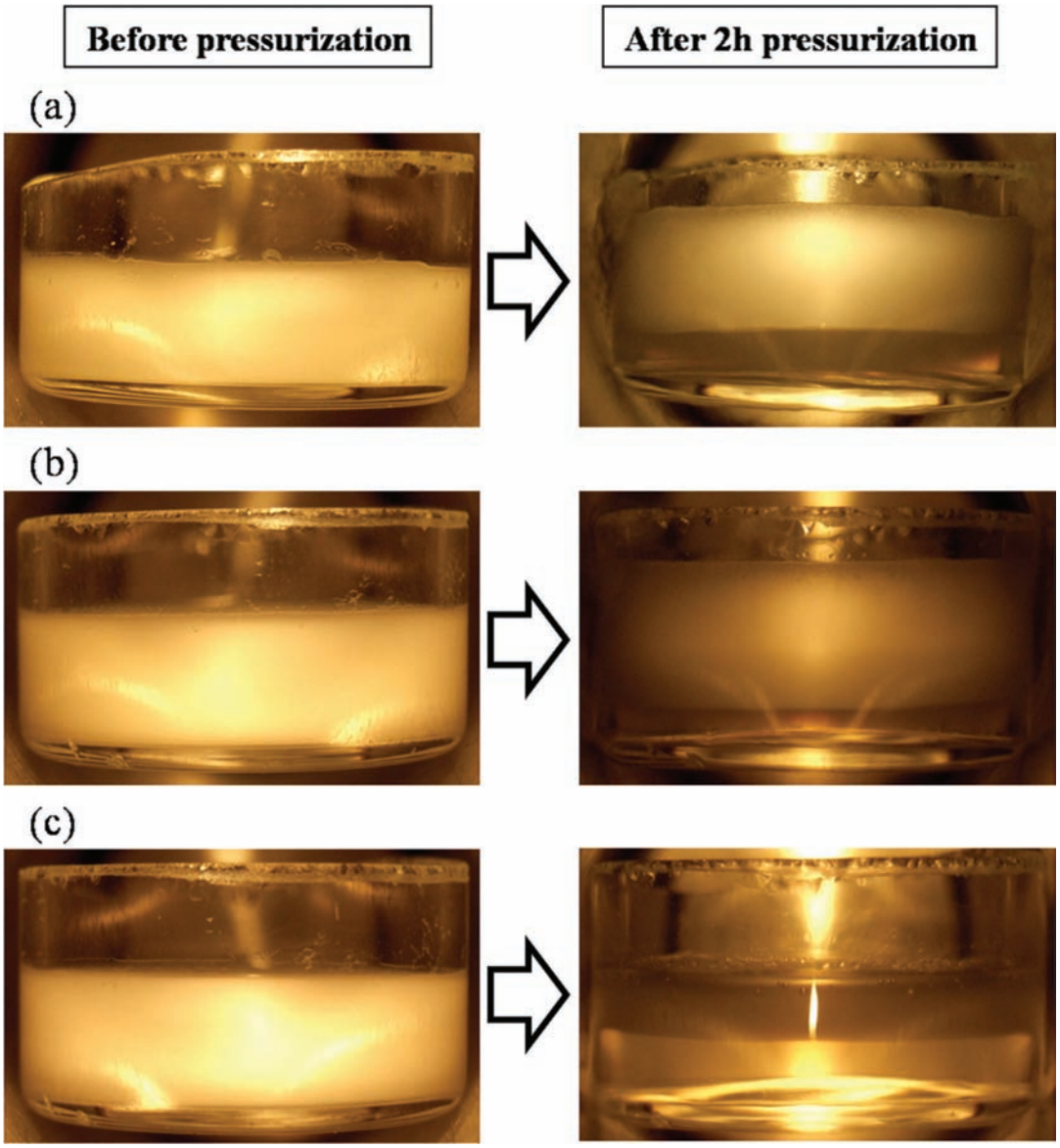

Fig. 1. Photo images of the emulsions before and after the processing with high-pressure CO_2 at 50°C and 10 MPa, (a) decane; (b) dodecane; (c) hexadecane. The processing time was 2 h.

As could be seen from the figure, the white-cloudy emulsion separated into the clear lower phase (water-rich phase) and the white-cloudy upper phase (creaming layer) by the pressurization with CO_2. By comparison, in case that the O/W emulsion was left still for 2 h at 50°C at ambient condition, obvious change was not observed (Fig. 7a). Therefore, it confirmed that this rapid phase separation is attributed to the deed of the high-pressure CO_2.

These results indicate that it is possible to demulsify the O/W emulsions with using high-pressure CO_2. From the figure, it is also clear that the smaller the carbon number of the oil, the larger the volume of the upper oil phase.

It is presumably due to the increase in the solubility of CO_2 in the oil with the decrease in the carbon number of alkanes, which results in the increase in volume of the oil phase in the emulsion. As the high expansion of the oil phase volume may influences the experimental results, further experiments were conducted with hexadecane as the oil phase.

Fig. 2 shows the photo images of hexadecane before (a) and after 2 h of pressurization with CO_2 at 50°C and at pressures up to 10 MPa (b–f). As could be seen from the figure, the higher the pressure of CO_2, the larger the degree of the volume change of hexadecane.

Fig. 3 shows the photo images of the aqueous solution of Tween 20 (i.e., the aqueous phase of the

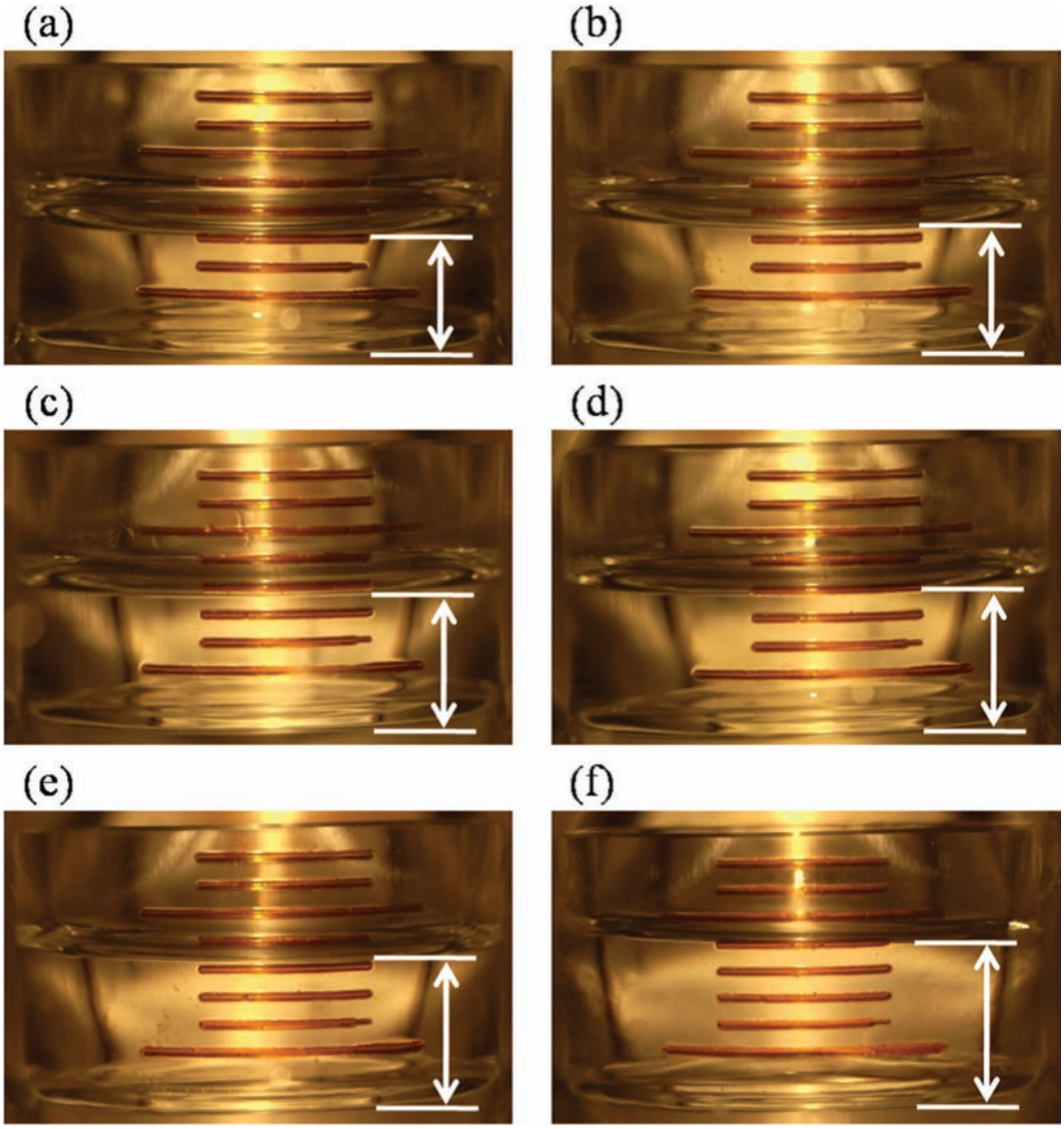

Fig. 2. Photo images of hexadecane before (a) and after 2 h of pressurization with CO_2 at 50°C and pressures up to 10 MPa (b–f). (a) Before pressurization, (b) 2 MPa; (c) 4 MPa; (d) 6 MPa; (e) 8 MPa; (f) 10 MPa.

emulsion) before (left) and after 2 h of pressurization with CO_2 at 50°C and 10 MPa (right). The volume of the surfactant solution hardly changed after the pressurization.

From Figs. 2 and 3, it could be concluded that the pressurization with CO_2 causes the swelling of the oil phase, and results in the increase in density difference between the oil phase and the aqueous phase. This increase in density difference will induces the acceleration of flotation of the oil droplets in the emulsion.

Fig. 4 shows the time course of the expansion coefficient of hexadecane under high-pressure CO_2 at 50°C and at pressures up to 10 MPa. The expansion coefficient was calculated according to the following equation.

$$\beta = \frac{\Delta V}{V_0} \times 100[\%], \tag{3}$$

where β [%] is the expansion coefficient, ΔV [cm^3] is the increase in the volume of hexadecane under high-pressure CO_2, and V_0 [cm^3] is the volume of hexadecane before pressurization.

From the figure, it is clear that the expansion of hexadecane was completed within about 10 min. This result indicates that diffusion of CO_2 into hexadecane and following expansion completes within 10 min.

The density of hexadecane under high-pressure CO_2 was calculated using the expansion volume and

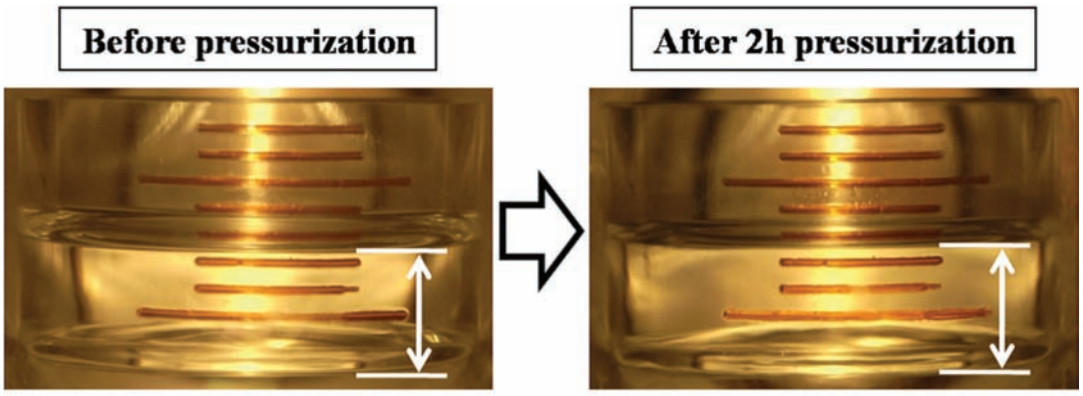

Fig. 3. Photo images of the aqueous solution of Tween 20 before (left) and after 2 h of pressurization with CO_2 at 50°C and 10 MPa (right).

the density of CO_2 according to the following equation with the following assumption:

1. The volume change of hexadecane under pressure is caused by the dissolution of CO_2 into hexadecane.
2. The molar volume of CO_2 doesn't change in hexadecane.
3. Hexadecane does not dissolve into CO_2.

$$\rho_p = \frac{M_0 + \rho_{CO_2}\Delta V}{V_0 + \Delta V}. \quad (4)$$

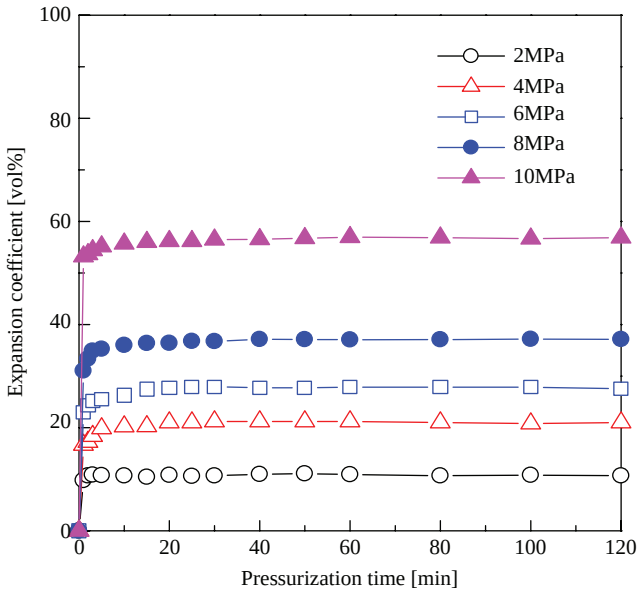

Fig. 4. Time course of the expansion coefficient of hexadecane under high-pressure CO_2 with 50°C, each pressure (2–10 MPa). (○) 2 MPa, (△) 4 MPa; (□) 6 MPa; (●) 8 MPa and (▲) 10 MPa.

In Eq. (4), ρ_p [g cm^{-3}] is the density of hexadecane under high-pressure CO_2, M_0 [g] is the mass of hexadecane before pressurization, ρ_{CO2} [g cm^{-3}] is the density of CO_2, ΔV [cm^3] is the increase in the volume of hexadecane under pressure, and V_0 [cm^3] is the volume of hexadecane before pressurization. The density of CO_2 at 50°C was calculated with an accurate equation of state [12], and shown in Table 1.

Fig. 5 shows the expansion coefficient of hexadecane and the density of hexadecane under high-pressure CO_2. The expansion coefficient increased with the increase in pressure.

From the expansion coefficient and the density of hexadecane under high-pressure CO_2, floatation rate ratio, or the ratio of the flotation rate of the O/W emulsion droplet under high-pressure CO_2 to that under the ambient condition 50°C under atmospheric pressure), was evaluated by Eq. (6) with the following assumptions:

1. Stokes' equation (5) could be adapted under high-pressure CO_2.
2. The density of the aqueous phase of the O/W emulsion does not change under high-pressure CO_2.

Table 1
Density of CO_2 at 50°C

Temperature [°C]	Pressure of CO_2 [MPa]	Density of CO_2 [g cm^{-1}]
50	2	0.0355988
50	4	0.0788582
50	6	0.1352086
50	8	0.2191840
50	10	0.3843289

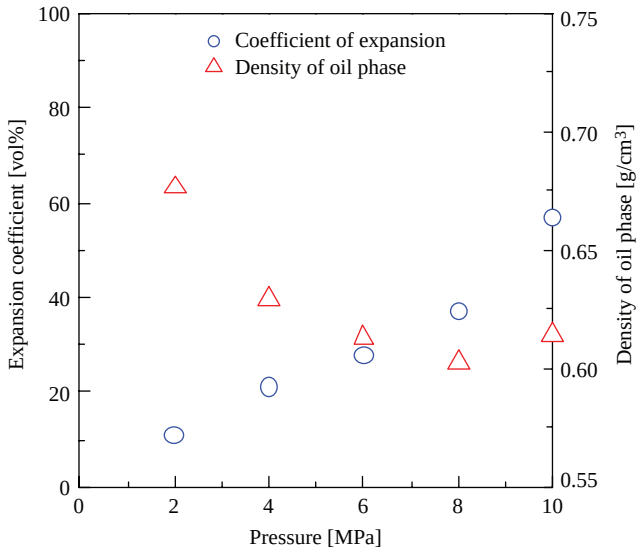

Fig. 5. Pressure dependence of the expansion coefficient of hexadecane (△) and the density of hexadecane under high-pressure CO_2 (○).

3. Aggregation of the oil droplet does not take place during the flotation. The droplet diameter depends only on the expansion ratio.

$$v_s = \frac{D_p^2(\rho_f - \rho_p)g}{18\eta}. \quad (5)$$

$$\text{Flotation} - \text{rate ratio} = \frac{v_s,\ \text{under pressure}}{v_s,\ \text{abbient}}, = \frac{(1+\beta/100)^{2/3} \times (\rho_f - \rho_p)_{\text{under pressure}}}{(\rho_f - \rho_p)_{\text{abbient}}} \quad (6)$$

where v_s [cm s^{-1}] is the flotation rate of the oil droplet in the O/W emulsion, D_p [cm] is the diameter of the oil droplet, ρ_f [g cm^{-3}] is the density of the aqueous phase, ρ_p [g cm^{-3}] is the density of the oil phase, g [cm s^{-2}] is the gravity acceleration, and η [Pa s] is the viscosity of the aqueous phase.

The floatation rate ratio was adopted because the calculation of the exact flotation rate of the oil droplet under high-pressure CO_2 is difficult because the droplet size is unknown [13].

Fig. 6 shows the flotation-rate ratio of the hexadecane droplet. It should be noted that the flotation-rate ratio is 1.0 [–] at 50°C and under atmospheric pressure.

From the figure, it is clear the floating rate of the droplet swollen by the CO_2 is faster than that without CO_2. In the real systems, increase in the flotation rate would be more significant due to the swelling of the oil droplet by CO_2.

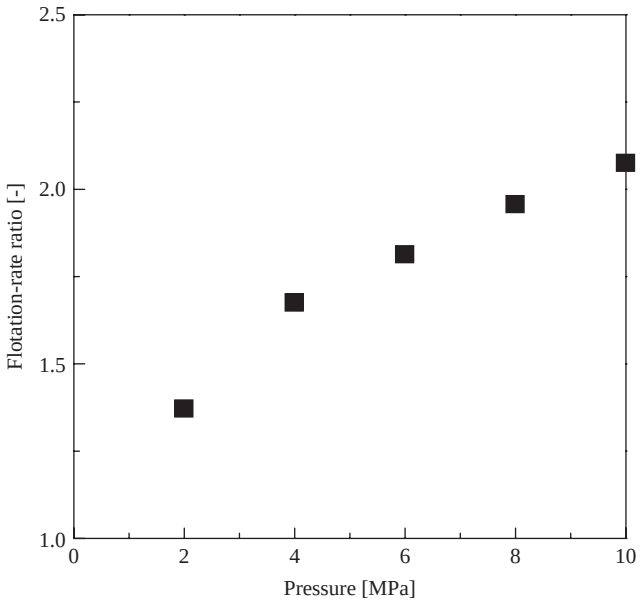

Fig. 6. Flotation-rate ratio of the hexadecane droplet based on the Stokes' equation. The flotation-rate ratio is 1.0 [–] at 50°C under atmospheric pressure.

Fig. 7 shows the photo images of the hexadecane O/W emulsions under various pressures at 50°C after 2 h. The clarity of the lower phase of the hexadecane emulsion increased with the increase in pressure. As described above, this fact could be explained by the increase of the droplet flotation rate with the increase in pressure.

3.2. Electrical conductivity

In this study, the electrical conductivity was measured to observe the behavior of creaming of the O/W emulsion under high-pressure CO_2. As the electrical conductivity of the oil phase is much lower than that of the aqueous phase, the electrical conductivity of the lower phase increases with the floatation of the oil droplet. Therefore, the rate of increasing in electrical conductivity corresponds to the rate of creaming.

Fig. 8 shows the time course of the electrical conductivity of the O/W emulsions and Tween 20 solution under high-pressure CO_2. For the case of the Tween 20 solution, the electrical conductivity rapidly increased to the saturation value within 100 min after the pressurization. On the other hand, in the case of the O/W emulsions, the electrical conductivity increased slowly, and not reached to the conductivity of the Tween 20 solution within the time range of this study. In addition, except for just after the pressurization, the smaller the carbon number of the oil, the higher the electrical conductivity of the emulsion. It is presumably due to the fact that the decrease in the alkane carbon number of oil causes increase in the solubility of CO_2, and then

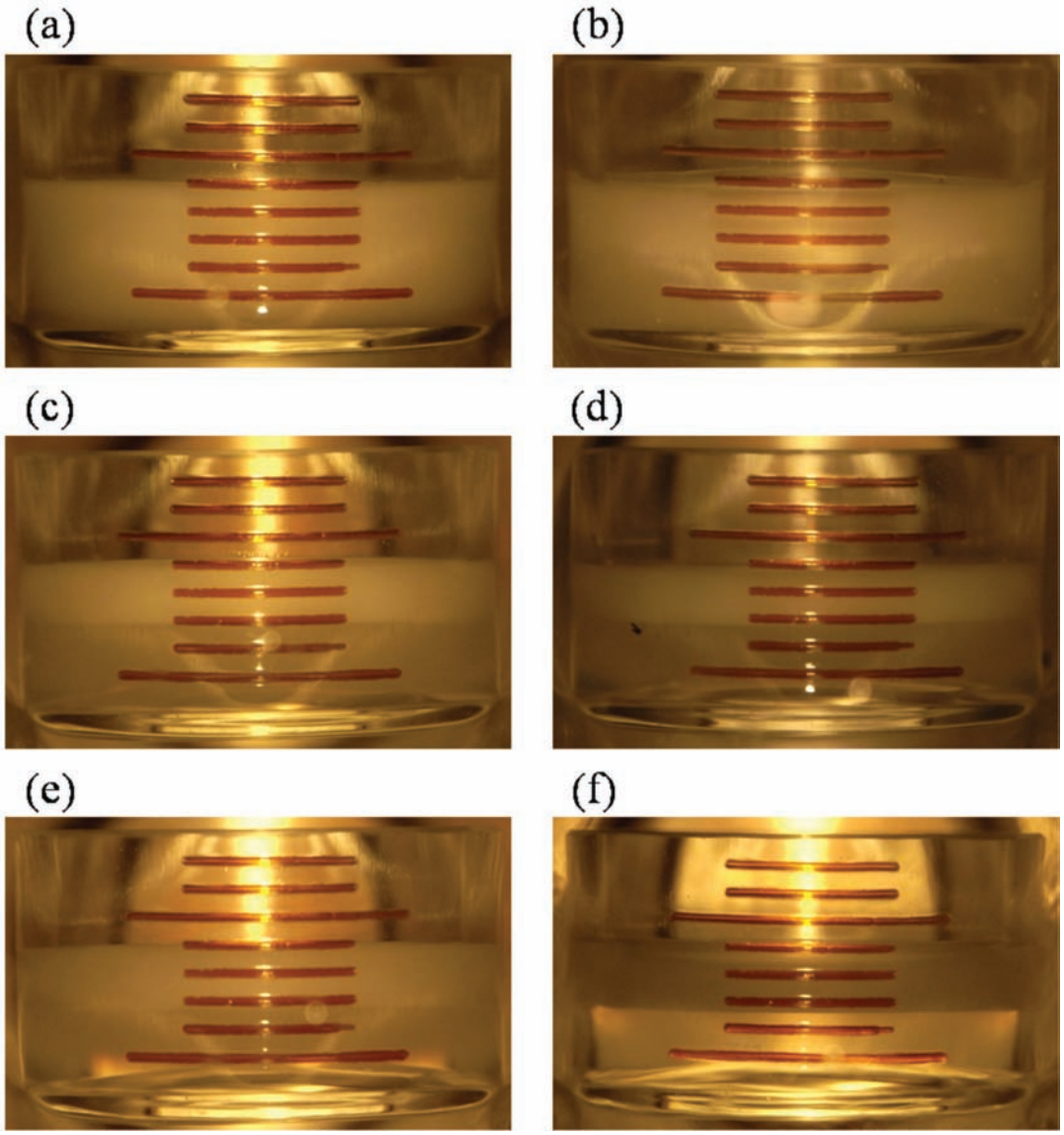

Fig. 7. Photo images of the hexadecane emulsions under high-pressure CO_2 at 50°C after 2 h. (a) Before experiment, (b) atmospheric pressure; (c) 4 MPa; (d) 6 MPa; (e) 8 MPa and (f) 10 MPa.

accelerates the decrease in density of the oil phase. As a result of the decrease in the oil phase density, the concentration of the oil droplets in the lower phase decreases by the flotation of the oil droplets.

3.3. Demulsification efficiency

In this study, the demulsification of the hexadecane O/W emulsion was conducted with three different procedures as follows:

Method 1: Static method.
The O/W emulsion was pressurized by CO_2 without stirring, and left still during the demulsification period.

Method 2: Stirring method.
The O/W emulsion was pressurized by CO_2 with stirring. After the pressurization, the emulsion was stirred for 10 min with a stirring tip at the bottom of the glass cell. Then, the stirring was stopped, and the emulsion left still for the demulsification.

Method 3: Bubbling method.
The O/W emulsion was pressurized up to 8 MPa similar to the static method. Then, CO_2 was further fed to the autoclave from the bottom of the emulsion by bubbling. After the pressure reached to 10 MPa, the bubbling was stopped, and the emulsion left still for the demulsification.

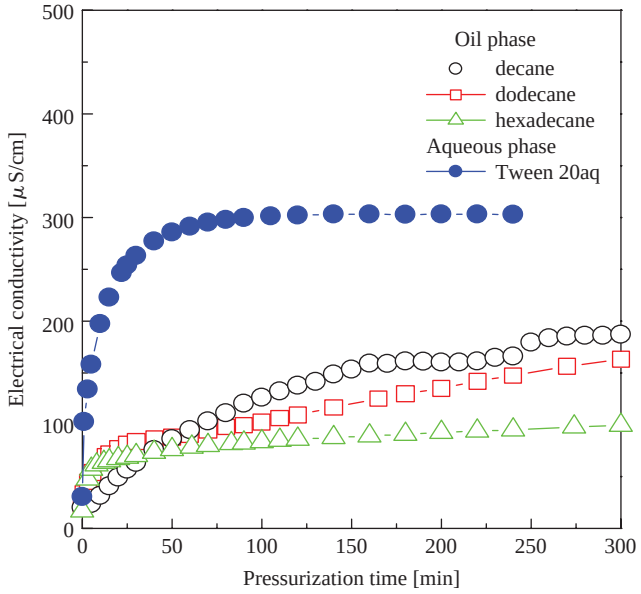

Fig. 8. Time course of the electrical conductivity of the lower phase of the emulsions: decane (○), dodecane (□), hexadecane (△), and Tween 20 solution (●) (aqueous phase of emulsions) at 50°C and 10 MPa.

Fig. 9 shows the demulsification efficiency for Method 1. It could be seen from the figure that the ϕ_{oil} decreased rapidly at first though, the change became small for the longer time. This behavior qualitatively corresponds to the electrical conductivity of the lower aqueous phase of the hexadecane emulsion. These facts could be attributed to the diffusion resistance of the upper phase (i.e., the oil rich creaming layer which formed after the pressurization) for CO_2. The initially formed creaming layer inhibits the diffusion of CO_2 to the lower phase, which results in the slow flotation of the emulsion droplets in the lower phase.

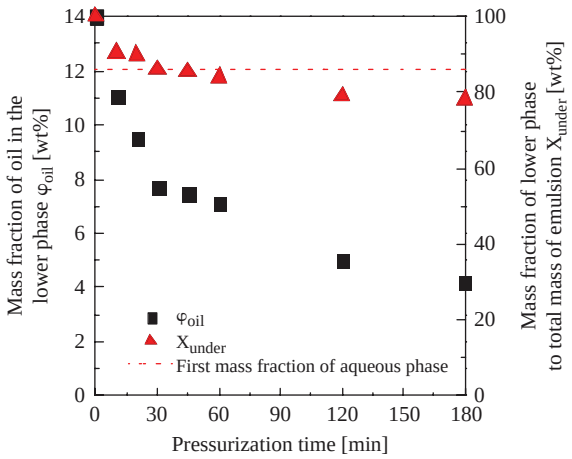

Fig. 9. Time course of the ϕ_{oil} (■) and the X_{under} (▲) of the hexadecane emulsion in the case of Method 1. (50°C, 10 MPa)

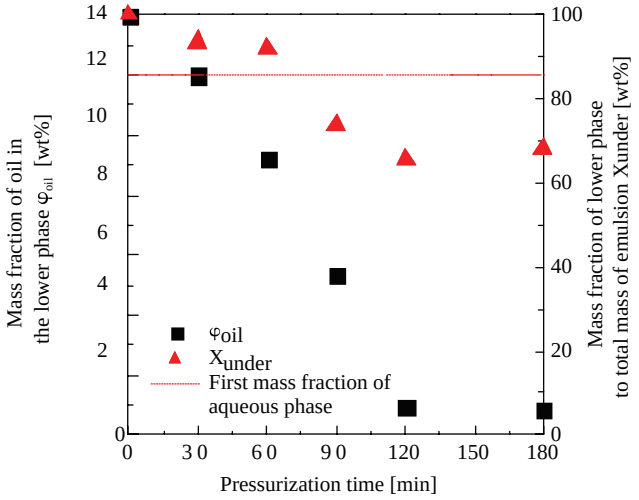

Fig. 10. Time course of the ϕ_{oil} (■) and the X_{under} (▲) of the hexadecane emulsion in the case of Method 2. (50°C, 10 MPa)

In addition, as expected, the mass fraction of the lower layer X_{under} also decreased with the formation of the creaming layer. However, the X_{under} does not reach to the 86%, the theoretical limit. This fact suggests that water was absorbed into the gap between the oil droplets in the creaming layer, and could not be recovered from the emulsion.

Fig. 10 shows the demulsification efficiency for Method 2. This stirring method is constructed from the stirring step and the resting step. These steps will have following effect, respectively.

Stirring step: The diffusion of CO_2 into the lower phase and the dissolution of CO_2 into the oil droplets are accelerated by breaking the creaming layer with stirring.

Resting step: The formation of the creaming layer is accelerated by leaving the emulsion at rest.

As shown in the figure, the rapid decrease of the ϕ_{oil} lasted for 2 h. Compared with Method 1, the ϕ_{oil} was initially higher in the short time range (up to an hour) though, the ϕ_{oil} decreased to less than 1 wt%. The initial stage could be explained by the breakage of the emulsion droplet due to the stirring, which inhibits the floatation.

Fig. 11 shows the demulsification efficiency for Method 3. This bubbling method has the CO_2 bubbling step at the pressurizing period and the resting step. The CO_2 bubbling step will have the following effects.

1. The diffusion of CO_2 into the lower phase and the dissolution of CO_2 into the oil droplets are accelerated by feeding CO_2 in the form of bubble.

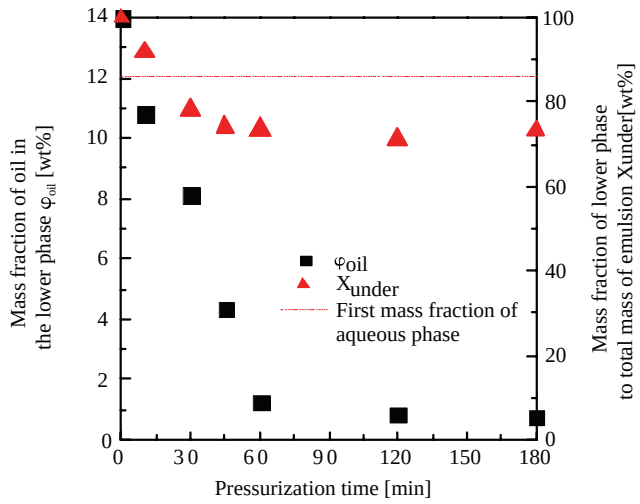

Fig. 11. Time course of the ϕ_{oil} (■) and the X_{under} (▲) of the hexadecane emulsion in the case of Method 3. (50°C, 10 MPa)

2. As the bubbling is conducted slowly, the diffusion of CO_2 is accelerated without breaking the creaming layer and the droplet breakage.

As shown in the figure, the ϕ_{oil} was rapidly decreased compared with the other two methods, and reached to about 1 wt% after 1 h of the pressurization. The demulsification efficiency was dramatically improved with the bubbling.

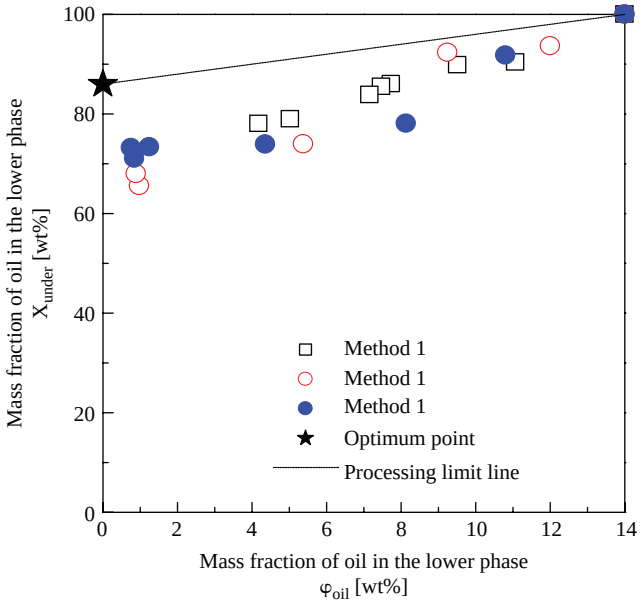

Fig. 12. The plot of the X_{under} versus the ϕ_{oil} of the hexadecane emulsion in the case of demulsifying by each method under high-pressure CO_2 with 50°C, 10 MPa. (□) Method 1, (○) Method 2; (●) Method 3 and (★) Optimum point.

Fig. 12 shows the plot of the X_{under} versus the ϕ_{oil} of the hexadecane O/W emulsion obtained in this study. As shown in the figure, Method 3 is the most close to the optimum point (theoretical limit) of the three methods. The discrepancy between the theoretical limit and the experimental results suggests the existence of water trapped between the oil droplet in the creaming layer. In addition, the facts that the X_{under} is roughly proportional to the ϕ_{oil} and their slope was similar to each other for all three methods indicate that the coalescence of the oil droplets hardly happened in this demusification process.

4. Conclusions

In this study, a new process for the demulsification of O/W emulsion with high-pressure CO_2 was proposed. For the confirmation of the concept, the demulsification of the model O/W emulsion formed with a nonionic surfactant, Tween 20, was conducted. Experimental results show that the pressurization with CO_2 is hopeful for the new demulsification process.

Symbols

X_{under}	Mass fraction of lower phase to total mass of emulsion, wt%
ϕ_{oil}	Mass fraction of oil in the lower phase, wt%
ΔH_{oil}	Heat of melting of oil per gram of the emulsion, J
H_{oil}	Heat of melting per gram of oil, J g^{-1}
β	Expansion coefficient, vol%
ΔV	Expansion volume, cm^3
V_0	Volume of hexadecane before pressurization, cm^3
v_s	Flotation rate of oil droplet, cm s^{-1}
D_p	Diameter of oil droplet, cm
ρ_f	Density of aqueous phases, g cm^{-3}
ρ_p	Density of oil phase, g cm^{-3}
g	Gravity acceleration, cm s^{-2}
η	Viscosity of aqueous phase, Pa s

References

[1] M. Shields, R. Ellis and B.R. Saunders, Coll. Surf. A: Physicochem. Eng. Asp., 178 (2001) 265–276.
[2] D. Allende, A. Cambiella, J.M. Benito, C. Pazos and J. Coca, Chem. Eng. Technol., 31(7) (2008) 1007–10014.
[3] B.P. Binks, R. Murakami, S.P. Armes and S. Fujii, Langmuir, 22 (2006) 2050–2057.
[4] Y. Fan, S. Simon and J. Sjoblom, Energy Fuels, DOI: 10.1021/ef900355d.
[5] Y.B. Zhou, L. Chen, X.M. Hu and J. Lu, Ind. Eng. Chem. Res., 48 (2009) 1660–1664.
[6] T. Ichikawa, K. Itoh and S. Yamamoto, Coll. Surf. A: Physicochem. Eng. Asp., 242 (2004) 21–26.

[7] Y. De Smet, L. Deriemaeker, E. Parloo and R. Finsy, Langmuir, 15 (1999) 2327–2332.
[8] P.J. Dale, J. Kijlstra and B. Vincent, Coll. Surf. A: Physicochem. Eng. Asp., 291 (2006) 85–92.
[9] T. Skodvin and J. Sjoblom, J. Coll. Interf. Sci., 182 (1996) 190–198.
[10] M. Clausse, Coll. Polym. Sci., 255 (1977) 40–44.
[11] T. Hanai, Emulsion Science, in: P. Sherman (Ed), Academic Press (1968).
[12] R. Span, W. Wagner, Lehrstuhl fur Thermodynamik, Ruhr-Universitat Bochum, D-44780 Bochum, Germany.
[13] R. Chanamai and D.J. McClements, Coll. Surf. A: Physicochem. Eng. Asp., 172 (2000) 79–86.